Spin asymmetries in elastic and in elastic scattering from rubidium

W E Guinea[1], G F Hanne[1,2], M R Went[1,5], M L Daniell[1], M A Stevenson[1], K Bartschat[3], D Payne[3], W R MacGillivray[1,4] and B Lohmann[1]

[1] Centre for Quantum Dynamics, Griffith University, Nathan, Qld 4111, Australia

[2] Physikalisches Institut, Universitat M¨unster, Wilhelm-Klemm-Str. 10, 48149 M¨unster, Germany

[3] Physics Department, Drake University, Des Moines, IA 50311, USA

[4] Faculty of Sciences, University of Southern Queensland, Toowoomba, Qld 4350, Australia

E-mail: B.Lohmann@griffith.edu.au

Received 10 May 2005 Published 5 September 2005

J. Phys. B: At. Mol. Opt. Phys. 38(2005) 3359–3366 doi:10.1088/0953-4075/38/18/007

Abstract

Experimental and theoretical results are presented for the A_2 spin asymmetry for elastic and inelastic scattering of spin-polarized electrons from rubidium, at incident electron energies of 15, 20, 30, 50 and 80 eV. Theoretical calculations are performed within a semi-relativistic Breit–Pauli *R*-matrix (close-coupling) model. The experimental data reveal significant asymmetries at all energies. The experimental results are reasonably well described by the present theoretical calculations and by other calculations using a relativistic distorted-wave approach, and provide a clear relativistic signature.

Introduction

Spin-resolved electron–atom collision experiments provide a stringent test of theoretical models of the scattering process. This is exemplified by recent theoretical results from Andersen and Bartschat (2002). They investigated inelastic electron scattering from heavy alkalis and found that the standard (not spin-resolved) Stokes parameters, such as those derived from electron–photon coincidence or superelastic scattering experiments, are insensitive to relativistic effects in the scattering process. This explains why, for example, the collision parameters obtained by Karaganov *etal*(2002) from superelastic scattering measurements on Cs were very well described by a (non-relativistic) convergent close-coupling (CCC) calculation, even though one would expect relativistic effects to play a role in such a heavy target. Andersen and Bartschat recommended measurement of the *generalized Stokes parameters*, which involve the use of polarized electron and/or atom beams. For example, they showed that the spin-asymmetry parameters A_1 and A_2, which are identically zero in a nonrelativistic (LS-coupled) approximation, exhibit significant non-zero values when calculated in a semi-relativistic Breit–Pauli *R*-matrix model. This prediction was confirmed by comparison with experimental data from Baum *etal*(2004), who recently performed a systematic study of the behaviour of the ‘exchange asymmetry’ A_{nn}, the ‘spin–orbit asymmetry’ A_2 and the ‘interference asymmetry’ A_1 for 6s $\rightarrow$6p excitation of Cs. In particular, they observed significant non-zero A_2 spin asymmetries.

Recently published measurements (Hall *etal*2004) of 'standard' collision parameters for 5s →5p excitation in Rb have also been in generally good agreement with CCC calculations. However, it is clear that spin-resolved measurements are required in order to unambiguously determine whether relativistic effects are actually significant in this process. To this end, we have measured the A_2 asymmetry parameter for scattering of spin-polarized electrons from unpolarized Rb atoms. The measurements have been performed at incident energies of 15, 20, 30 and 50 eV, for both elastic and inelastic scattering and at 80 eV for elastic scattering. Theoretical calculations have been performed using a semi-relativistic Breit–Pauli *R*-matrix model. The numerical method used in the calculations is described below, however, full details of the model may be found in Payne *etal*(2005). The experimental data are compared with the latter calculations and with results from a relativistic distorted-wave calculation (Zeman *etal*1998, Stauffer 2003).

Experimental details

The spin-polarized electron spectrometer used in these measurements has been described in detail in a previous publication (Went *et al* 2002). Here we present a brief overview of the apparatus. The spin-polarized electron source is a wafer of crystalline GaAs, which is treated with Cs and O_2 to produce a negative electron affinity surface. Spin-polarized electrons are photoemitted from the surface after illumination with circularly polarized 810 nm radiation from a laser diode. The handedness of the incident radiation can be reversed using a liquid crystal retarder, resulting in emission of 'spin-up' or 'spin-down' electrons. The emitted electrons pass through a 90◦ electrostatic deflector, before being guided via an electron optical train into the scattering chamber. The electron beam entering the scattering chamber is thus transversely spin polarized, with the electron spin being perpendicular to the scattering plane. A two-stage oven is used to produce a beam of rubidium atoms; the interaction region is formed by the intersection of the atom and electron beams, with the atom beam lying in the same plane as the incident and scattered electrons. The rubidium atoms are trapped on the far side of the interaction region by a LN_2 cooled cold trap. Scattered electrons are energy analysed by a hemispherical electron energy analyser, which can be rotated in the scattering plane through an angular range of 30◦–110◦. The spin-asymmetry parameter for scattering of polarized electrons from unpolarized atoms, A_2, is determined by measuring the number of scattered electrons, N, emitted at a given scattering angle, for spin-up (↑) and spin-down (↓) orientations of the incident electrons.

One can write

$$A_2P = \frac{N\uparrow - N\downarrow}{N\uparrow + N\downarrow} = S_AP, \quad (1)$$

where S_A is the standard left–right (or spin up–down) asymmetry function (Kessler 1985) for inelastic scattering of spin-polarized electrons from a beam of unpolarized atoms and P is the degree of spin polarization of the incident electron beam. In our apparatus, the degree

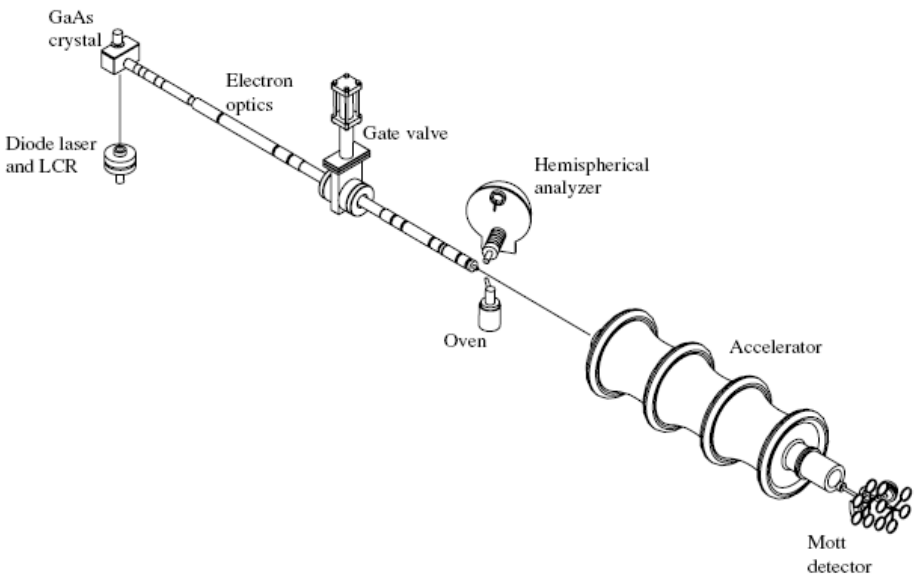

Figure 1. Schematic diagram of the spin-polarized electron spectrometer.

of spin polarization may be measured using a Mott polarimeter (Kessler 1985) or by reference to published asymmetry functions for Xe (M¨uller and Kessler 1994). The degree of spin polarization ranges from 20% to 35%, depending upon the particular GaAs crystal. A schematic diagram of the apparatus is presented in figure 1.

The data acquisition procedure is as follows. For a given incident energy, the number of electrons scattered at a particular angle was measured repeatedly (approximately 100 times) for spin-up orientation and spin-down orientation of the incident electrons. The collection time at each spin orientation was 10 s. Many scans (up to 100) through the entire accessible angular range (from 30◦ to 110◦) were performed in order to obtain the final data set.

The energy calibration for the scattered electron energy analyser was obtained by measurement of the $M_{4,5}N_{2,3}N_{2,3}$ krypton Auger lines (Werme *et al* 1972) in the 50–55 eV region and the autoionization lines in Rb at lower energies (Pejˇcev *et al* 1977). The angular calibration of the scattered electron analyser was achieved by measuring the critical minimum in the elastic cross section for elastic scattering of unpolarized electrons from argon at 60 eV (Panajotovi´c *et al* 1997).

Figure 1. Schematic diagram of the spin-polarized electron spectrometer.

Numerical method

The semi-relativistic *R*-matrixmethod based upon amodified version of the computer program of Berrington *et al* (1995) was used in the calculation performed for this work. We began with a five-state model (labelled BP5 below) including the $(5s)^2S_{1/2}$, $(5p)^2P_{1/2,3/2}$ and $(4d)^2D_{3/2,5/2}$ physical target states. The next more extensive 12-state model (BP12) then included the additional seven states $(6s)^2S_{1/2}$, $(6p)^2P^0_{1/2,3/2}$, $(5d)^2D_{3/2,5/2}$ and $(4f)^2F^0_{3/2,5/2}$, respectively.

The target description was based upon a model potential for the inner 36 core electrons. It was constructed using the Hartree potential generated from the Rb^+ orbitals of Clementi and Roetti (1974), supplemented by polarization and exchange potentials as described by Albright *et al* (1993). Using the program COREPOT of Bartschat (1996), excellent agreement with experiment was achieved for the ionization potentials of all valence orbitals, the electron affinity of Rb^- and the dipole polarizability of Rb. Finally, relativistic effects were accounted for, in part, by explicitly adding the one-electron spin–orbit term to both the N-electron target and the $(N + 1)$-electron collision Hamiltonian before diagonalization. In addition, optimizing the core potential effectively accounts for the spin-conserving mass correction and Darwin terms.

In order to check the convergence of the close-coupling expansion with the number of coupled states, we then followed the procedure outlined by Bartschat and Fang (2000) and generated pseudo-orbitals and the corresponding states [core]*nl*, where *nl* denotes the pseudoorbital.

In the BP19 model, we added one s, p, d and f orbital and, consequently, seven more states to the trial function of the close-coupling expansion, while the biggest approximation (BP37) contained 37 states built with pseudo-orbitals up to $11s$, $10p$, $8d$ and $7f$. These orbitals were generated by enforcing orthogonality of a Sturmian expansion for each orbital to all physical orbitals. An exponential fall-off parameter of 0.88 was chosen in this expansion to ensure a similar range of the pseudo-orbitals as the physical orbitals (5s and 5p) for the transitions of interest. For reasons of both available computational resources and numerical stability, we did not increase the close-coupling expansion any further. However, experience with the *R*-matrix with pseudo-states (RMPS) method suggests that the results will generally converge well with the number of states in the close-coupling expansion, and this expectation is supported by the current results (see below). Finally, we note that only the BP5 model was pushed to projectile energies of 50 and 80 eV. The high energy of the basis functions needed was achieved by using a smaller *R*-matrix radius *a* that only encompasses the 5s, 5p and 4d orbitals. For the BP5 model, we used $a = 30$ au, while the other models required $a = 50$ au. Depending on the partial-wave symmetry, we used up to 50 continuum orbitals per orbital angular momentum of the projectile electron and calculated results for total electronic angular momenta up to $J = 40$ of the collision system numerically. Even then it was necessary to use a geometric extrapolation scheme to estimate contributions from the higher partial waves in order to get a smooth angular dependence of the parameters of interest. Since the experiment does not resolve the individual fine-structure states, the results for excitation of the 5p states were obtained by summing up the contributions from both levels, weighted by the respective differential cross sections. Note that the 'fine-structure effect' can produce non-zero spin asymmetries if the individual fine-structure levels are resolved (Hanne 1976). A zero spin asymmetry would be obtained, however, if one averages over the fine-structure levels. Hence, the observation of a non-zero spin asymmetry for the fine-structure-averaged case is a clear sign of relativistic effects. The only relativistic effect accounted for in the numerical method described here is the one-electron spin–orbit interaction; observation of a non-zero asymmetry would thus be a strong indication that this is the dominant relativistic effect.

Results and discussion

The asymmetry function S_A can be written in terms of the spin-up, spin-down differential cross sections as (Kessler 1985)

$$S_A = \frac{(\sigma\uparrow - \sigma\downarrow)}{(\sigma\uparrow + \sigma\downarrow)}. \quad (2)$$

The above equation illustrates that particularly high asymmetry values can arise at those energies and angles where there is a deep minimum in the differential cross section, and the

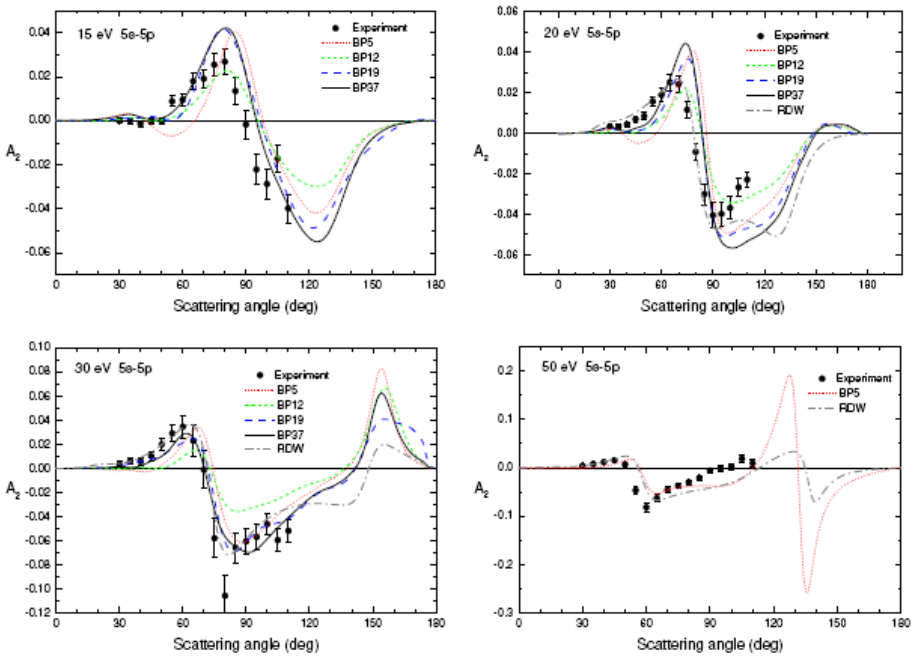

Figure 2. Experimental and theoretical A_2 parameter for 5s to 5p excitation of Rb, at incident energies of 15, 20, 30 and 50 eV. The various calculations are described in the text.

spin-up cross section is displaced from the spin-down cross section by, for example, the different spin–orbit interactions. Such points are often called 'critical points' and the calculations of the spin asymmetry at such points are very sensitive to the details of the interaction (for example, charge-cloud polarization and exchange and correlation effects).

Figures 2 and 3 present the experimental and theoretical results for the A_2 parameter for inelastic 5^2S to 5^2P excitation of, and for elastic scattering from, unpolarized rubidium atoms. The energy resolution in the current measurements was approximately 400 meV, sufficient to readily resolve the energy loss peak associated with 5s–5p excitation from other spectrum features. The A_2 parameter has been measured for inelastic scattering at incident energies of 15, 20, 30 and 50 eV, while the elastic scattering measurements have been performed at each of the latter energies and also at 80 eV. The cross section for inelastic scattering was too small to permit a measurement of the asymmetry at this energy. The various theoretical calculations are labelled as follows: Breit–Pauli five-state calculation—BP5, Breit–Pauli 12-state calculation—BP12, Breit–Pauli 19-state calculation (with pseudo-states)—BP19, Breit–Pauli 37-state calculation (with pseudo-states)—BP37 and relativistic distorted wave—RDW. The RDW calculations of Stauffer and co-workers are included for inelastic scattering at incident energies of 20, 30 and 50 eV. The BP5–BP37 calculations have been performed for inelastic and elastic scattering at 15, 20 and 30 eV. At higher energies (50 and 80 eV), only the BP5 calculation was computationally feasible.

The first thing to be noted in the experimental data is that significant asymmetries are present at all energies, for both elastic and inelastic scattering. This represents a clear signature of relativistic effects. The level of agreement between theory and experiment is

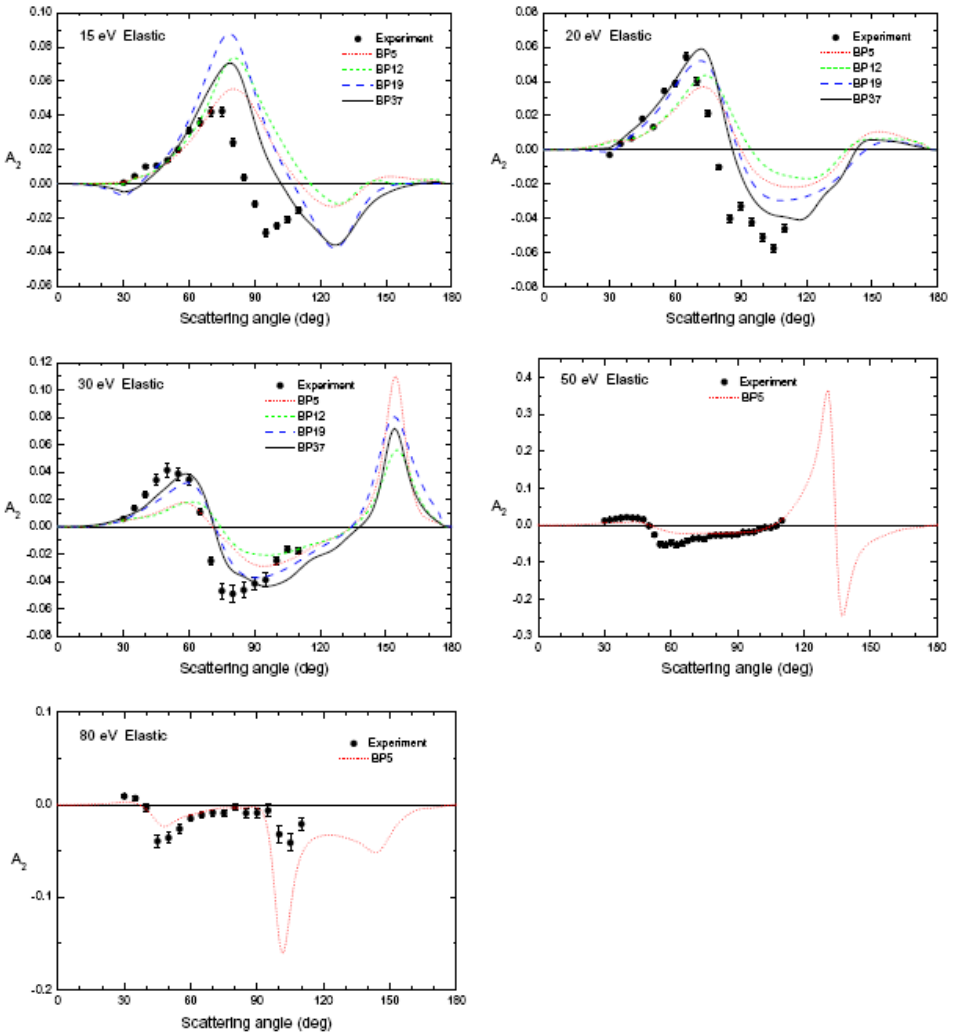

Figure 3. Experimental and theoretical A_2 parameter for elastic scattering from ground-state Rb, at incident energies of 15, 20, 30, 50 and 80 eV. The various calculations are described in the text.

variable. We first consider the RDW calculation for inelastic scattering (figure 2). There is remarkably good agreement with the experimental data for the 5s–5p asymmetry at 20 and 30 eV incident energies. At 50 eV incident energy, there is also good agreement in terms of the magnitude of the asymmetry, but there is a distinct angular shift of the theory relative to the experiment.

For elastic scattering, the BP5, BP12, BP19 and BP37 *R*-matrix calculations show a distinct convergence of the results as the number of states is increased. Interestingly, for the case of inelastic scattering (figure 2), the BP5, BP19 and BP37 show very similar features, but are quite different to the BP12 calculation. For the case of 5s–5p inelastic scattering, the BP37 model generally overestimates the magnitude of the asymmetry. As the incident energy increases, there is an increasing discrepancy in the angular position of the first positive asymmetry peak and the first negative asymmetry peak, with each peak occurring at a larger angle than is observed experimentally. At an incident energy of 50 eV, the BP5 and RDW calculations are quite similar at forward angles and give a reasonable representation of the magnitude of the asymmetry, if not the angular positions of the various features.

For the case of elastic scattering (figure 3), no RDW calculations are available. The present BP37 calculations are in good agreement with the experimental data, in terms of magnitude, at 20 and 30 eV, but there are some discrepancies at 15 eV. There is also an angular offset between the theoretical predictions and the experimental data at each energy. At higher energies (50 and 80 eV), the experimental results are compared with a BP5 calculation, and there is quite good agreement. At 80 eV, the pronounced minimum in the asymmetry

seen in the calculations at 100◦ is not reproduced in the experiment. We have calculated the asymmetry after convolution of the spin-up/spin-down theoretical differential cross sections with the experimental angular resolution of ±2◦. Although the depth of the 'dip' in the asymmetry is reduced (from –0.16 to –0.14), there is still a considerable discrepancy with experiment. The results indicate that the theoretical calculation underestimates the magnitude of the minimum in the differential cross section near 100◦.

It is of interest to compare the experimentally determined A_2 parameter for inelastic and elastic scattering, at the same incident energy. Generally, the magnitude of the asymmetry for excitation and for elastic scattering is very similar (with the asymmetry for elastic scattering being generally somewhat larger in the region of the first positive peak). A similar trend is apparent when comparing the spin-asymmetry data of Baum *et al* (2004) for inelastic scattering from Cs, with their previous measurements (Baum *et al* 2002) for elastic scattering from Cs. The similarity between the elastic and inelastic asymmetries can be explained by the fact that the one-electron spin–orbit interaction in the incident channel is the dominant interaction, once the fine-structure effect is excluded. In this model, the inelastic process is considered as a two-step process (for example, scattering from the target and then energy loss) in which the field of the final excited-state atom is not substantially different to that of the ground-state atom. One would expect this assumption to break down at very low energies, where the excitation energy becomes significant compared to the incident energy. Indeed, the experimental data tend to support this argument, with the differences between the inelastic and elastic asymmetries being greater at the lower incident energies.

Generally, the RDW calculation appears to perform well, although the calculations are only available for a small number of energies, and only for inelastic scattering. The level of agreement with the Breit–Pauli calculations we have presented is generally good. The largest discrepancy between the BP37 model and experiment, for the magnitude of the asymmetry, occurs at lower energies. At higher energies, the (relatively simple) BP5 performs quite satisfactorily, except at the incident energy of 80 eV, where the calculation appears to significantly underestimate the magnitude of the differential cross section in the region of the cross section minimum near 100◦, resulting in large asymmetry values. Further calculations, using a variety of models, seem highly desirable to resolve the remaining discrepancies.

Acknowledgments

This work was supported by the Australian Research Council. WEG would like to acknowledge the assistance of an Australian Postgraduate Award and GFH would like to acknowledge the support of the Volkswagen Stiftung. Finally, KB and DP acknowledge support from the United States National Science Foundation under grant PHY-0244470.

References

Albright B J, Bartschat K and Flicek P R 1993 *J. Phys. B: At. Mol. Opt. Phys.* **26** 337
Andersen N and Bartschat K 2002 *J. Phys. B: At. Mol. Opt. Phys.* **35** 4507
Bartschat K 1996 *Computational Atomic Physics* (Heidelberg: Springer)
Bartschat K and Fang Y 2000 *Phys. Rev.* A **62** 052719
Baum G, F¨orster S, Pavlovi´c N, Roth B, Bartschat K and Bray I 2004 *Phys. Rev.* A **70** 012707
Baum G, Pavlovi´c N and Roth B 2002 *Phys. Rev.* A **66** 022705
Berrington K A, Eissner W B and Norrington P N 1995 *Comput. Phys. Commun.* **92** 290
Clementi E and Roetti C 1974 *At. Data Nucl. Data Tables* **14** 177
Hall B V, Shen Y, Murray A J, Standage M C, MacGillivray W R and Bray I 2004 *J. Phys. B: At. Mol. Opt. Phys.* **37** 1113
Hanne G 1976 *J. Phys. B: At. Mol. Phys.* **9** 805
Karaganov V, Teubner P J O and Brunger M J 2002 *Correlations, Polarization and Ionization in Atomic Systems* ed D H Madison and M Schultz (New York: American Institute of Physics) p 19
Kessler J 1985 *Polarized Electrons* (Berlin: Springer)
M¨uller H and Kessler J 1994 *J. Phys. B: At. Mol. Opt. Phys.* **27** 5893
Panajotovi´c R, Filipovi´c D, Marinkovi´c, Pej˘cev V, Kurepa M and Vuškovi´c L 1997 *J. Phys. B: At. Mol. Opt. Phys.* **30** 5877

Payne D, Krueger B and Bartschat K 2005 *J. Phys. B: At. Mol. Opt. Phys.* **38** 3349
Pej˘cev V, Rassi D, Ross K J and Ottley T W 1977 *J. Phys. B: At. Mol. Phys.* **10** 1653
Stauffer A D 2003 private communication
Went M R, McEachran R P, Lohmann Birgit and MacGillivray W R 2002 *J. Phys. B: At. Mol. Opt. Phys.* **35** 4885
Werme L O, Bergmark T and Siegbahn K 1972 *Phys. Scr.* **6** 141
Zeman V, McEachran R P and Stauffer A D 1998 *Eur. Phys. J.* D **1** 117